Coral symbiotic algae calcify *ex hospite* in partnership with bacteria

Jörg C. Frommlet[a,b,1], Maria L. Sousa[a,b], Artur Alves[a,b], Sandra I. Vieira[c,d,e], David J. Suggett[f], and João Serôdio[a,b]

[a]Department of Biology, [b]Center for Environmental and Marine Studies (CESAM), [c]Autonomous Section of Health Sciences, [d]Center for Cell Biology, and [e]Institute for Biomedicine, Santiago Campus, University of Aveiro, 3810-193 Aveiro, Portugal; and [f]Functional Plant Biology & Climate Change Cluster, University of Technology Sydney, Broadway, NSW 2007, Australia

Dinoflagellates of the genus *Symbiodinium* are commonly recognized as invertebrate endosymbionts that are of central importance for the functioning of coral reef ecosystems. However, the endosymbiotic phase within *Symbiodinium* life history is inherently tied to a more cryptic free-living (*ex hospite*) phase that remains largely unexplored. Here we show that free-living *Symbiodinium* spp. in culture commonly form calcifying bacterial–algal communities that produce aragonitic spherulites and encase the dinoflagellates as endolithic cells. This process is driven by *Symbiodinium* photosynthesis but occurs only in partnership with bacteria. Our findings not only place dinoflagellates on the map of microbial–algal organomineralization processes but also point toward an endolithic phase in the *Symbiodinium* life history, a phenomenon that may provide new perspectives on the biology and ecology of *Symbiodinium* spp. and the evolutionary history of the coral–dinoflagellate symbiosis.

Symbiodinium | coral symbiont | microbial–algal calcification | endolithic algae | life history

Dinoflagellates of the genus *Symbiodinium* form symbiotic relationships with corals, other marine invertebrates, and protists and are considered keystone species in coral reef ecosystems (1–3). In symbiosis, *Symbiodinium* spp. provide their hosts with photosynthates in exchange for host-derived metabolites, and *in hospite* of scleractinian corals they also enhance coral calcification, the biomineralization process that provides the structural framework for the entire coral reef ecosystem (4–6). However, members of this genus also are found *ex hospite* both in the water column and the benthos (7, 8). These free-living *Symbiodinium* populations encompass both obligate and temporary free-living phylotypes, and it is well established that the latter represent an important pool for the horizontal acquisition of symbionts by coral juveniles (2, 9). In fact, free-living populations of otherwise symbiotic phylotypes are increasingly recognized as central to maintaining coral functional diversity and ultimately reef ecosystem viability (10, 11), but the biology and ecology of these symbiotic and obligate free-living *Symbiodinium* populations in the environment remain largely unknown.

Coral calcification stems from the coral itself but in symbiotic (hermatypic) species is enhanced by the photosynthetic activity of their symbionts through a process termed "light-enhanced calcification" (4–6). Involvement of *Symbiodinium* spp. in this biomineralization process is quite unusual, because, apart from a small number of free-living species that form calcified cysts (calcispheres), dinoflagellates generally are not considered to be important biomineralizers (12, 13). A more primitive mineralization process that has shaped our planet over billions of years is organomineralization (14–17). This type of mineralization involves an organic matrix as a precipitation template and is driven either by extrinsic factors such as evaporation or degassing (biologically influenced organomineralization) or by biological activity (biologically induced organomineralization) (18, 19). One of the most important biologically induced organomineralization processes throughout Earth's history is microbially induced

carbonate formation (14–19). Several metabolic pathways are known to drive microbially induced calcification, but oxygenic photosynthesis is considered the most significant (14–17, 19). Cyanobacteria and to a much lesser extent diatoms, as well as brown, green, and red microalgae, have been identified as the key phototrophic partners within these calcifying microbial–algal communities (14–17, 19). Dinoflagellates have been found within calcifying communities (20, 21), but whether they actively drive calcification has never been addressed. Here we show that free-living *Symbiodinium* spp. in culture commonly form calcifying bacterial–algal biofilms with naturally associated bacteria. We provide a morphological and ultrastructural description of these calcifying biofilms, present an elemental analysis of their mineral phase, and demonstrate that the calcification process is driven by the photosynthetic activity of *Symbiodinium* but, to occur, also requires naturally associated bacterial communities. We present the first report, to our knowledge, of a dinoflagellate being the phototrophic driver in a calcifying microbial–algal biofilm and provide evidence for an endolithic phase in the *Symbiodinium* life history. This finding demonstrates the need to reevaluate not only the role of dinoflagellates in organomineralization but also the life history dynamics of *Symbiodinium* and the coral–dinoflagellate symbiosis that is the foundation of coral reef ecosystems.

Results

Discovery of Organomineralization in *Symbiodinium* Cultures. The basis for this study was the incidental discovery of circular

Significance

The dinoflagellate genus *Symbiodinium* is best known for harboring important endosymbiotic algae of marine invertebrates, notably reef-building corals. However, these dinoflagellates also live freely within coral reef waters and sediments and provide an important environmental pool for the colonization of new coral recruits. Although *Symbiodinium* facilitate coral calcification indirectly when *in hospite*, we show that they also can calcify in partnership with bacteria when free living. This discovery offers entirely new perspectives on fundamental questions regarding the life cycle and ecology of these dinoflagellates and could help explain how changes in ocean chemistry created a selective pressure that ultimately led *Symbiodinium* to establish an endo-symbiotic life style. To our knowledge, our findings document the first identified dinoflagellate–bacterial calcifying community.
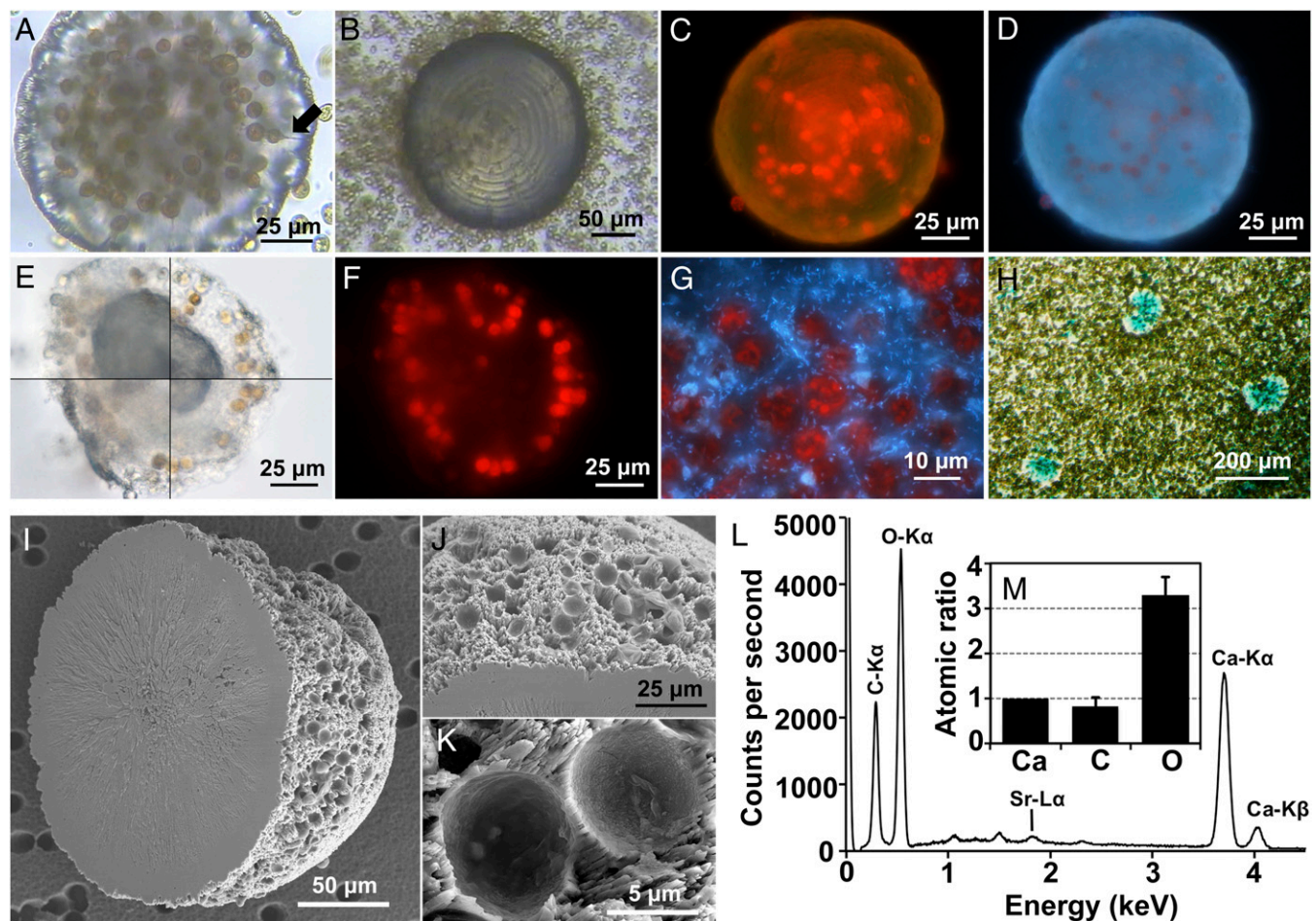
Fig. 1. Morphology, biota, ultrastructure, and elemental composition of symbiolites. (*A*) Symbiolite in *Symbiodinium* culture 362. The arrow highlights one of the ducts observed in focal plane (see also Movie S1). (*B*) Symbiolite in culture 24 with well-defined growth rings. (*C*) Red chlorophyll fluorescence of embedded *Symbiodinium* cells and green symbiolite fluorescence under blue-light (450–490 nm) excitation. (*D*) Blue fluorescence of symbiolites when excited with UV light (330–380 nm). (*E*) Acid digestion of a symbiolite in 30-s steps, clockwise from upper left. (*F*) The symbiolite in *E* after acid digestion. Chlorophyll fluorescence demonstrates how the *Symbiodinium* cells are held in place by the remaining matrix. (*G*) Blue fluorescence of bacteria after acid digestion and DAPI staining (culture 203). (*H*) Positive staining of symbiolite-associated EPS with Alcian blue. (*I*–*M*) SEM micrographs of a symbiolite without biota and EPS. (*I*) Symbiolite showing the overall hemispherical shape and the round depressions left by the removed algal cells. (*J* and *K*) Detailed views of features shown in *I*. (*L* and *M*) Elemental composition of the symbiolite mineral phase as determined by EDS. (*L*) Annotated energy dispersion spectra. (*M*) Atomic ratios of calcium (Ca), carbon (C), and oxygen (O) based on their K-series spectra ($n = 3$).

structures of unknown nature within our culture collection of *Symbiodinium* spp. that encompassed a large extent of known genetic diversity (Table S1) (22, 23). The discovered structures were up to 150–200 μm in diameter, firmly attached to the culture vessels, virtually transparent, and contained numerous *Symbiodinium* cells in their coccoid stage, many of which appeared to be connected to the structures' surface through ducts (Fig. 1*A* and Movie S1). The structures themselves often displayed well-defined concentric growth rings (Fig. 1*B*) and when excited with blue or UV light displayed green or blue fluorescence, respectively (Fig. 1 *C* and *D*). Blue and UV light also excited chlorophyll fluorescence in the embedded algal cells (Fig. 1 *C* and *D*), a first sign for their viability that later was confirmed by measurements of their photosystem II (PSII) maximum quantum yield [variable fluorescence/maximum fluorescence (F_v/F_m) = 0.40 ± 0.07 SD], which was not significantly different from that of cells in the same culture but outside the structures (F_v/F_m = 0.42 ± 0.04 SD) ($n = 6$, *t* test, $P = 0.25$).

To test whether these structures were a living organism that somehow might have contaminated our unialgal cultures rather than an organic or inorganic formation, we performed a series of tests. Addition of HCl resulted in the partial dissolution of the structures

with effervescence, an indication of the presence of a carbonate mineral, but left the structural outline intact because a malleable matrix or tissue remained (Fig. 1 *E* and *F*). DNA staining of acid-digested samples to visualize any eukaryotic nuclei gave no evidence for a complex cellular tissue, suggesting an organic nature of the matrix itself, and revealed a high abundance of prokaryotes associated with the matrix (Fig. 1*G*). Further, positive Alcian blue staining showed that the structure-associated matrix contained acidic polysaccharides (Fig. 1*H*) (24), which are common components of extracellular polymeric substances (EPS) and play an important role in organomineralization (19). Together, these properties consistently indicated that the structures were an organomineral (18, 19).

Ultrastructure and Composition of the Mineral Phase. Scanning electron microscopy (SEM) of structures from which the biofilm had been removed showed that the mineral phase was composed of orthorhombic crystals in an acicular crystal habit, producing hemispherical spherulites (Fig. 1*I*). The spherulite base was generally planar and smooth (Fig. 1*I*), whereas their spherical surface was rough and covered with round depressions where the removed dinoflagellate cells had been located (Fig. 1 *J* and *K*). As shown below,
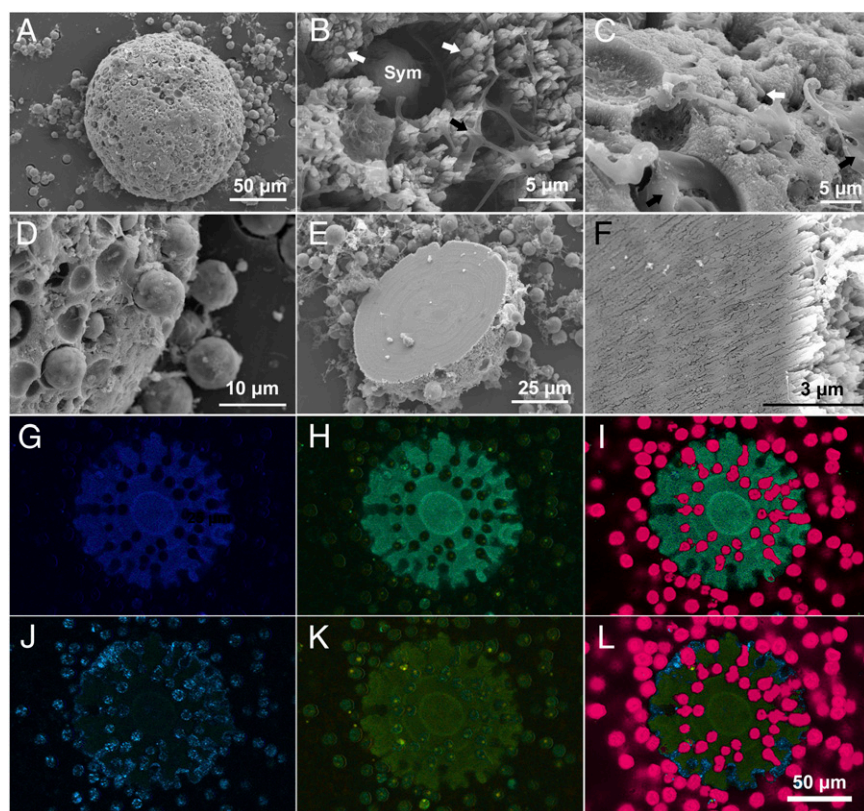
Fig. 2. Symbiolite ultrastructure and fluorescence properties of live, undisturbed symbiolites. (*A*) SEM micrograph of a symbiolite in top view showing the EPS coating and attached *Symbiodinium* cells. (*B* and *C*) SEM micrographs showing the weblike and membranous EPS (black arrows), *Symbiodinium* (Sym) partially encased in aragonite, and rod-shaped bacteria associated with the mineral phase (white arrows). (*D*) *Symbiodinium* cells at different stages of becoming encased in the symbiolite. (*E* and *F*) Symbiolite base with well-defined growth rings and needle-like aragonite crystals. (*G–I*) CLSM micrographs of symbiolite fluorescence properties when excited at 405 nm. (*G*) Blue aragonite fluorescence, 427–481 nm. (*H*) Green aragonite fluorescence, 492–620 nm. (*I*) Blue and green aragonite fluorescence and red chlorophyll fluorescence, 427–727 nm. (*J–L*) CLSM micrographs of symbiolite fluorescence properties when excited at 488 nm. (*J*) Blue biofilm fluorescence, 459–502 nm. (*K*) Blue biofilm and green aragonite fluorescence, 459–609 nm. (*L*) Blue biofilm, green aragonite, and red chlorophyll fluorescence, 459–727 nm. Magnification is identical in *G–L*.

the formation of these spherulites is driven by *Symbiodinium* spp., and thus we termed and hereafter refer to them as "symbiolites." Energy-dispersive X-ray spectroscopy (EDS) further revealed that symbiolites consisted of calcium, carbon, and oxygen [98.7% ± 0.2 SD (*n* = 3)] at an atomic ratio of ~1Ca:1C:3O, identifying the carbonate as calcium carbonate ($CaCO_3$) (Fig. 1 *L* and *M*). Other detectable elements included strontium at a Ca:Sr ratio of 1:0.0086 ± 0.0001 SD, which, together with the orthorhombic crystal system, established that symbiolites were aragonitic (25).

Structural Organization of the Bacterial–Algal Biofilm and the Mineral Phase. SEM of osmium tetroxide (OsO_4)-fixed symbiolites was used to study the microstructure of the biofilm in relation to the mineral phase (Fig. 2 *A* and *F*). Two types of EPS were discernible, a weblike type between the aragonite crystals and a membranous type that covered the symbiolite surface (Fig. 2 *A–C*). The dinoflagellate cells were associated mainly with the outer side of the membranous EPS matrix and were captured in different stages of becoming surrounded by the growing mineral phase (Fig. 2 *A*, *B*, *D*, and *E*). SEM showed only a few bacteria that mainly were associated with the mineral surface (Fig. 2 *B* and *C*). Considering the high abundance of bacteria detected using DAPI staining (Fig. 1*G*), this apparent scarcity suggests that the majority of the bacterial community was embedded in the EPS matrix and thus was undetectable by SEM. In addition to the biofilm components the symbiolite in Fig. 2 *E* and *F* displays well-defined growth rings and the acicular arrangement of the aragonite crystals described above.

Confocal laser-scanning microscopy (CLSM) performed directly in the culturing vessels without disturbing the culture gave further insight into the structural organization of the living biofilm and the mineral phase in the natural state. Excitation with near-UV light (405 nm) induced both blue and green fluorescence emissions from the aragonitic mineral phase and red chlorophyll fluorescence from *Symbiodinium* that peaked around 680 nm (Fig. 2 *G–I*). The aragonite fluorescence (Fig. 2 *G* and *H*; overlaid with chlorophyll

fluorescence in Fig. 2*I*) confirmed that the duct-like features that had been observed under the light microscope were indeed channels in the mineral phase through which endolithic cells remained connected to the external environment. Excitation with blue light (488 nm) induced blue EPS fluorescence, green aragonite fluorescence, and red chlorophyll fluorescence (Fig. 2 *J–L*). EPS fluorescence (Fig. 2*J* and overlaid with aragonite and chlorophyll fluorescence and in Fig. 2 *K* and *L*) showed that symbiolites, including the *Symbiodinium*-containing invaginations inside the mineral phase, were coated in a continuous layer of EPS and that EPS also covered *Symbiodinium* cells outside of symbiolites.

Symbiolite Growth and Reversibility of the Endolithic Phase. Since their discovery we have found symbiolites in 92.5% of all *Symbiodinium* strains examined, and noncalcifying cultures were not specific to any single phylotype or culture origin (*n* = 40; Table S1). To assess if commonly used artificial culturing media also would support calcification, we compared symbiolite formation in seawater-based f/2 medium with that in two types of artificial ASP-8A medium, one buffered with Tris and the other buffered with bicarbonate (Table S2). Total alkalinity (TA) of f/2 medium was within the expected range of natural surface seawater, which averages at ~2.37 meg/L (26). Tris-buffered ASP-8A had a TA that was ~280% higher than that of the f/2 medium, and bicarbonate-buffered ASP-8A had a TA that was more comparable to that of natural seawater (Table S2). During the 42-d study, more than 84% of the strains grown in f/2 medium and more than 51% of the strains in bicarbonate-buffered ASP-8A but none of the strains in Tris-buffered ASP-8A calcified (Table S2).

Symbiolite growth and the associated embedding of *Symbiodinium* cells into the aragonite deposit were studied over several consecutive light/dark cycles using time-lapse photography (Fig. 3*A* and Movie S2). Quantitative image analysis showed that calcification was light-dependent and thus was driven by the photosynthetic activity of *Symbiodinium* (Fig. 3*B*). Also noticeable was that symbiolite growth
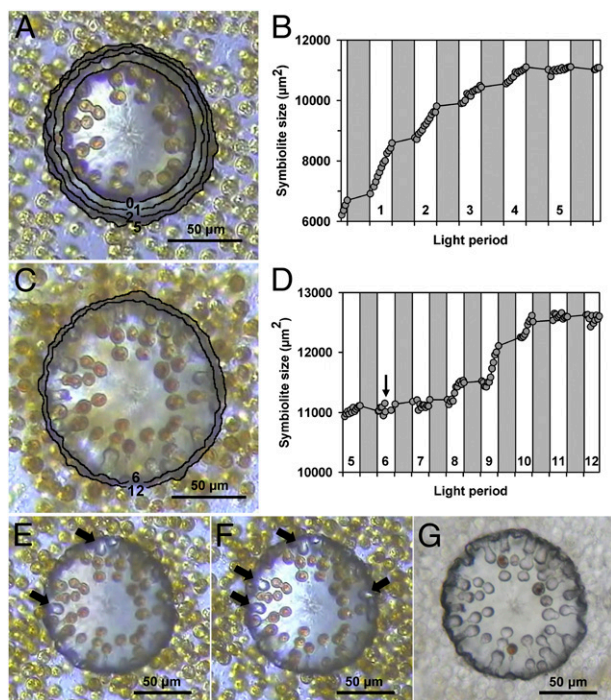
Frommlet et al.

Fig. 3. Symbiolite growth dynamics. (*A*) Symbiolite growth over five consecutive light/dark periods (numbered outlines show symbiolite size at the end of the respective light period; see also Movie S2). (*B*) Growth dynamics of the symbiolite shown in *A*. (*C* and *D*) Effect of medium exchange on symbiolite growth. (*C*) Symbiolite growth over six consecutive light/dark periods following medium exchange. (*D*) Growth dynamics of symbiolite shown in *C*. The arrow marks the time of medium exchange. (*E–G*) Symbiolite on days 2 (*E*), 4 (*F*), and 14 (*G*) following medium exchange. Arrows indicate voids in the symbiolite where *Symbiodinium* cells had emerged.

slowed over consecutive light cycles (Fig. 3*B*), suggesting that in batch culture calcification ultimately was limited by the growth medium. A subsequent experiment in which symbiolite growth could be reestablished by replacing the growth medium supported this hypothesis (Fig. 3 *C* and *D*). More importantly, however, the medium exchange also caused endolithic cells to re-emerge actively from the symbiolites and to vacate the structures effectively over the course of 2 wk (Fig. 3 *E–G* and Movie S3).

Importance of Bacteria for the Formation of Symbiolites. To assess the role of bacteria in symbiolite formation, we suppressed bacterial growth with antibiotics. The majority of the 35 tested cultures grew well in the presence of antibiotics, but EPS were visibly reduced, and calcification was suppressed completely (Table S3). Thus, bacteria were the main EPS producers and were essential for the calcification process. To examine the role of bacteria further, we isolated and identified 12 bacterial strains from symbiolite-forming *Symbiodinium* cultures (Table S3). Two isolates, a previously undescribed species of *Neptunomonas* (*Neptunomonas phycophila*) (27) and a strain of *Pseudoalteromonas atlantica*, a bacterium first isolated from marine algae and known for its production of large amounts of EPS (28), were tested in bacteria-addition experiments. Culturing of antibiotics-treated *Symbiodinium* strains in antibiotics-free medium reinitiated calcification in 18.75% of cultures, suggesting that the previous antibiotics treatment had not produced fully axenic cultures but instead had inhibited bacterial growth sufficiently to suppress calcification. However, inoculation of antibiotic-free medium with the same antibiotic-treated *Symbiodinium* strains and *N. phycophila* induced calcification in 50% of the cultures, showing a trend for higher calcification (Fisher's exact test, $P = 0.0627$). A statistically significant increase of calcifying cultures

to 87.5% (Fisher's exact test, $P = 0.0001$) was observed when the antibiotic-treated *Symbiodinium* strains were inoculated with *P. atlantica* (Fig. S1 and Table S4).

Discussion

Our results show that free-living *Symbiodinium* spp. in culture commonly form calcifying bacterial–algal biofilms with naturally associated bacteria. The wide range of phylogenetic diversity as well as geographic and host origins of calcifying strains (22, 23) imply a broad potential for establishing calcifying microbial–algal communities within the genus *Symbiodinium*. Moreover, non-calcifying cultures were not specific to any single clade, internal transcribed spacer (ITS) type, or culture origin, and thus calcification potential is more likely to be related to differences among bacterial communities than to *Symbiodinium* phylotype. A combination of factors including photosynthetic rates, development of the bacterial population, and associated EPS production will have to be studied in detail to develop a mechanistic understanding of this calcification process. However, our current results already show that symbiolite formation is biologically induced and suggest that this organomineralization process is based on the same components and principles that govern calcification in other microbial–algal communities, notably that phototrophs (here *Symbiodinium* spp.) that increase the $CaCO_3$ saturation state via their photosynthetic activity and prokaryotes that produce a matrix of EPS which has ion-binding properties, provide nucleation points for crystallization and create the microenvironment in which photosynthesis-driven calcification can occur (17, 19, 29). Our view that symbiolite formation is driven by photosynthetic changes in the carbonate system is supported not only by the reported light-dependency of calcification but also by the complete suppression of calcification in Tris-buffered ASP-8A medium, because this medium has an extremely high buffering capacity that minimizes the influence of photosynthesis on the carbonate system (30, 31). That ASP-8A medium when buffered with bicarbonate did not suppress calcification in the same way further supports this view. The widespread use of Tris-buffered ASP-8A in the culturing of *Symbiodinium* (32) also may explain how symbiolite formation could remain hidden even in long-established cultures.

To our knowledge, symbiolite formation is the first documented case of a microbial–algal calcification process that is driven by a dinoflagellate and as such may represent a valuable new model for the study of microbial calcification processes. Estimates of how important such a *Symbiodinium*-driven calcification process could be to carbonate budgets would be premature; however, our culture-based findings, together with observations from nature that free-living *Symbiodinium* spp. occupy a benthic niche (7, 8) and that dinoflagellates are found in calcifying reef sediments (20, 21), indicate that *Symbiodinium* spp. and potentially other benthic dinoflagellates (33) actually may play an important role in biologically induced calcification processes.

A curious feature of symbiolites is that encased *Symbiodinium* cells remain connected to the external environment through ducts. The formation of these ducts is likely the result of an up-folding of the EPS matrix around the algal cells by the growing mineral phase until the outer, nonprecipitating side of the matrix meets and restricts further mineral precipitation. The mechanism(s) that enable *Symbiodinium* to vacate symbiolites are not yet clear, but the ability itself suggests that in nature symbiolite formation is not an ecological dead-end but rather comprises part of a temporary endolithic life-cycle strategy. From a functional perspective, symbiolite formation and the associated creation of an endolithic, benthic stage in the *Symbiodinium* life cycle could act as a refuge to increase the retention of *Symbiodinium* on reefs when *ex hospite* as well as a physical barrier against grazing (34). Further, the absorption of UV radiation by symbiolites may protect the endolithic cells from high-energy solar radiation while still permitting photosynthesis (35, 36), and the

described ducts may positively affect nutrient diffusion to the endolithic cells and facilitate sensing of the physicochemical conditions in the external environment. These features seem particularly important for a functional and reversible endolithic life-cycle phase.

Symbiodinium's entry into the endolithic stage as a physiologically active coccoid vegetative cell, which represents a dominant phase in the life cycle of *Symbiodinium* spp. and other symbiotic dinoflagellates but is only transient in most free-living dinoflagellate species (1, 37, 38), raises the question of whether a dominant coccoid vegetative stage originally could have represented an adaptation of *Symbiodinium* to an endolithic life history that later aided in entering the endosymbiotic milieu. The magnesium-inhibition hypothesis offers a novel view in this context (39); it postulates that rising Mg:Ca ratios in seawater since the mid-Cretaceous lowered Ca^{2+} availability to *Symbiodinium* and thereby created a strong selective pressure for these microalgae to enter an endosymbiotic environment. Mechanistically, the magnesium-inhibition hypothesis is based on the assumption that lowered Ca^{2+} availability negatively affects *Symbiodinium* photophysiology. Although such an effect on photosynthesis has not yet been tested in *Symbiodinium*, it is well established that Ca^{2+} concentrations and associated changes in the seawater $CaCO_3$ saturation state affected marine microbial carbonate abundance over geological times and that the decline of microbial carbonates since the late Cretaceous was caused not only by increased metazoan grazing pressure but also by lower Ca^{2+} concentrations and a decrease in seawater $CaCO_3$ saturation state (14, 15, 40). Symbiolite formation should be affected by these factors in the same way as other microbial calcification processes; therefore the process is likely to have been more prevalent in the geological past. This reasoning offers a unique hypothesis of how changes in ocean chemistry could have led to the evolution of *Symbiodinium* spp. toward the endosymbiotic lifestyle that made them a fundamental pillar of modern coral reef ecosystems.

Materials and Methods

Origin and Culturing of *Symbiodinium* Strains. *Symbiodinium* strains were obtained from Mark Warner (University of Delaware, Newark, DE) (Table S1) and were routinely maintained in f/2 medium (41), based on Atlantic seawater, collected at the coast near Aveiro, Portugal. If not stated otherwise, f/2 medium also was used for experimentation. For a comparison of calcification in f/2 and artificial media, two types of ASP-8A medium were prepared. ASP-8A buffered with Tris, which is one of the most commonly used media for the culturing of *Symbiodinium* spp (32), was formulated according to Blank (31). Bicarbonate-buffered ASP-8A was prepared according to Brading et al. (42). All cultures were grown at 26 °C and with a photon flux density of 130–150 µmol photons·m^{-2}·s^{-1} on a 12-h:12-h light:dark cycle. Stock cultures were subcultured monthly at a 1:40 ratio of culture to f/2 medium. Experimental cultures were inoculated at the same ratio and, depending on the required volumes, were grown either in flat-bottomed 24-well multiwell plates for suspended cell cultures (Sarstedt), which were sealed with parafilm to avoid evaporation, or culture flasks with vented caps for suspended cell cultures (Sarstedt).

Alkalinity Measurements. Total alkalinity of f/2 and ASP-8A media were determined by manual volumetric titration of 5-mL samples with 0.16 N-sulfuric acid under constant steering. The pH and temperature were measured using a pH meter with a SenTix41 probe (WTW). Titration data were analyzed using a Gran function plot method (43, 44) in the online version of the Alkalinity Calculator software (45).

Acid Digestion and DAPI and Alcian Blue Staining. In preparation for acid digestion, symbiolites were detached from the culture vessel using a cell scraper, were transferred to a microscope slide, and were covered with a coverslip. To acid digest the samples, HCl (0.5 M) was placed at the edge of the coverslip at a 10:1 ratio of sample to acid (final concentration, 50 mM). Staining with DAPI was performed overnight directly in the culture vessels at a final concentration of 0.4 µg/mL (46), followed by the acid-digestion protocol. Alcian blue staining was performed directly in the culture vessels for 30 min with 1.0% Alcian blue 8GX (Acros) in 3% acetic acid, pH 2.5 (47).

Light and Fluorescence Microscopy. Light and fluorescence microscopy were conducted on an Eclipse 80i epifluorescence microscope (Nikon) using the inbuilt

white and external mercury lamp light source (Model C-SHG1; Nikon). For documentation, a D5-2Mv digital sight camera (Nikon) was used. Symbiolite auto-fluorescence was studied using a blue filter (excitation, 470/40 nm; filter, 450–490 nm) (B-2A; Nikon) and a UV filter (UV-2B; Nikon; excitation, 355/50 nm; filter, 330–380 nm) (UV-2B; Nikon). DAPI staining was visualized using the UV-2B filter. For the study of undisturbed cultures (e.g., Alcian blue staining and time-lapse footage) an inverted Leica DM IL light microscope (Leica) was used (see *Time-Lapse Photography* below for details).

Measurements of Maximum PSII Quantum Yield. Photosynthetic activity of *Symbiodinium* cells inside symbiolites was confirmed by measuring the maximum quantum yield of PSII (F_v/F_m) in symbiolites that had been washed to remove cells attached to the outer surface. F_v/F_m also was measured in *Symbiodinium* cells not associated with symbiolites (i.e., deposited on the bottom of the culture vessel). Measurements were carried out using a pulse amplitude modulation fluorometer (48) comprising a control unit (Walz) and a WATER-EDF universal emitter-detector unit (Gademann Instruments) with a modulated blue light (an LED lamp peaking at 450 nm, half-bandwidth of 20 nm) as source for measuring actinic and saturating light (49). Fluorescence was measured using an optical-grade plastic optical fiber with a diameter of 100 µm (Edmund Optics), which was introduced directly into the culture vessels and positioned perpendicularly to symbiolites and control areas using an MM33 micromanipulator (Märtzhäuser). Alignment between fiber optics and symbiolites was confirmed visually, using a Leica DM IL inverted microscope. The fluorometer was zeroed against f/2 medium, and samples were dark-adapted for 15 min before measurements. A saturation pulse (0.6 s) was applied to measure minimum (F_o) and maximum (F_m) fluorescence and to determine F_v/F_m (48).

SEM/EDS. Samples for SEM/EDS were detached from the culture vessel using a cell scraper, transferred to a reaction tube, and processed either with or without OsO_4 fixation. Unfixed samples were prepared for the purpose of imaging the mineral phase and were washed twice with Milli-Q water by repeated pipetting, filtered onto polycarbonate filters with a pore size of 8 µm, and dried overnight at room temperature in a desiccator. OsO_4 fixations were performed for 10 min at a concentration of 2%. Fixed samples were filtered onto polycarbonate filters with an 8-µm pore size, washed with Milli-Q water for 20 min, and dehydrated over a period of 2 h in an increasing concentration of ethanol. The samples were critical-point dried in a Baltec CPD-030 (Balzers) and sputter-coated with gold-palladium. Both types of preparations were examined using an HR-FESEM Hitachi SU-70 scanning electron microscope with a QUANTAX 400 EDS spectrometer for elemental analysis (Bruker).

CLSM. Emission spectra of symbiolites were analyzed with the metadetector of an LSM-510 META confocal microscope (Zeiss) in Lambda mode. The following lasers and respective lines were used for culture excitation: a diode 405–430 laser with a 405-nm laser line and an Argon/2 laser with 458-, 477-, 488-, and 514-nm lines. The Lambda mode registers fluorescence emission between 411 and 754 nm in 10.7-nm intervals. Microphotographs of most relevant emission spectra were acquired with a PlanNeofluor 40×/1.3 oil objective and the HFT 405/488/633, using the 405-nm and the 488-nm lines alternatively at 100% of their power (30 mW). Emission quantitative data were obtained with the Zeiss LSM 510 4.0 software and were used to construct emission spectra profiles.

Time-Lapse Photography. For the study of symbiolite growth, cultures were grown on a Leica DM IL inverted light microscope. The light and temperature conditions in the incubator were replicated using an external light source (controlled to give a 12-h:12-h light:dark cycle) and the laboratory's air conditioning system. Time-lapse footage was recorded using a TK-C1481BEG video camera (JVC), was digitalized using a video capture device (Elgato), and was recorded with the Debut Video Capture Software (NCH Software). Measurements of symbiolite size were performed manually, using the freehand tool of the image analysis software ImageJ (US National Institutes of Health). Conversions from pixels to square micrometers were made using a calibration microscope slide (Leitz). Data points in Fig. 3 *B* and *D* are averages of three measurements. Time-lapse videos were created using the software VirtualDub (www.virtualdub.org/) at 25 frame/s. Captions were added using iMovie (Apple).

Isolation and Identification of Bacterial Strains. To isolate bacteria, biofilm and symbiolites of actively calcifying *Symbiodinium* cultures were detached from the culture vessel using a cell scraper, transferred to a reaction tube, and suspended by repeated pipetting. Several 50-µL aliquots of this homogenate were pipetted onto plates of Difco marine agar 2216 and were incubated at 25 °C until bacterial growth was evident (2–3 d). Bacteria were collected using

a loop and were streaked out on marine agar plates to isolate pure bacterial cultures. Resulting colonies were screened for morphological differences, and single colonies were identified by colony PCR using universal 16S rDNA primers 27F and 1492R (50). PCR products were purified using the DNA Clean and Concentrator-5 kit (Zymo Research) and were sequenced at GATC Biotech AG (Cologne, Germany). Sequences were read and edited with FinchTV 1.4.0 (Geospiza Inc., www.geospiza.com), and bacterial identification was done by searching against the Eztaxon database (www.ezbiocloud.net/eztaxon).

Antibiotics Treatments and Bacteria-Addition Experiments. Antibiotic treatments were carried out over a period of 6 mo by monthly subculturing with medium supplemented with tetracycline and streptomycin (Sigma) at a final concentration of 0.1 μg/mL each. Before each subculturing, the cultures were screened for symbiolites. Bacteria-addition experiments were conducted using these previously treated cultures. Three sets of cultures were inoculated 1:40 in 2 mL of f/2 medium without antibiotics, and a fourth set was subcultured into medium with antibiotics as before. Two of the three sets without

antibiotics then were inoculated with 20 μL of a suspension of *N. phycophila* or *P. atlantica*. The third set as well as the cultures with antibiotics received 20 μL of sterile seawater (control). Bacterial inoculates were prepared by resuspending several colonies grown overnight on marine agar plates in sterile seawater. Screening for calcification using an inverted microscope was performed over a period of 45 d on the days shown in Fig. S1.

1. Trench RK (1993) Microalgal-invertebrate symbioses: A review. *Endocytobiosis Cell Res* 9(2-3):135–175.
2. Stat M, Carter D, Hoegh-Guldberg O (2006) The evolutionary history of *Symbiodinium* and scleractinian hosts - Symbiosis, diversity, and the effect of climate change. *Perspect Plant Ecol Evol Syst* 8(1):23–43.
3. Baker AC (2011) Zooxanthellae. *Encyclopedia of Modern Coral Reefs: Structure, Form and Process*, ed Hopley D (Springer, Dordrecht, The Netherlands), pp 1188–1192.
4. Gattuso J-P, Allemand D, Frankignoulle M (1999) Photosynthesis and calcification at cellular, organismal and community levels in coral reefs: A review on interactions and control by carbonate chemistry. *Am Zool* 39(1):160–183.
5. Allemand D, et al. (2004) Biomineralisation in reef-building corals: From molecular mechanisms to environmental control. *C R Palevol* 3(6-7):453–467.
6. Tambutté S, et al. (2011) Coral biomineralization: From the gene to the environment. *J Exp Mar Biol Ecol* 408(1-2):58–78.
7. Littman RA, van Oppen MJH, Willis BL (2008) Methods for sampling free-living *Symbiodinium* (zooxanthellae) and their distribution and abundance at Lizard Island (Great Barrier Reef). *J Exp Mar Biol Ecol* 364(1):48–53.
8. Takabayashi M, Adams LM, Pochon X, Gates RD (2011) Genetic diversity of free-living *Symbiodinium* in surface water and sediment of Hawai'i and Florida. *Coral Reefs* 31(1):157–167.
9. Byler KA, Carmi-Veal M, Fine M, Goulet TL (2013) Multiple symbiont acquisition strategies as an adaptive mechanism in the coral *Stylophora pistillata*. *PLoS ONE* 8(3):e59596.
10. Abrego D, Willis BL, van Oppen MJH (2012) Impact of light and temperature on the uptake of algal symbionts by coral juveniles. *PLoS ONE* 7(11):e50311.
11. Pochon X, Putnam HM, Gates RD (2014) Multi-gene analysis of *Symbiodinium* dinoflagellates: A perspective on rarity, symbiosis, and evolution. *PeerJ* 2:e394.
12. Elbrächter M, et al. (2008) Establishing an Agenda for Calcareous Dinoflagellate Research (Thoracosphaeraceae, Dinophyceae) including a nomenclatural synopsis of generic names. *Taxon* 57(4):1289–1303.
13. Knoll AH (2003) Biomineralization and evolutionary history. *Rev Mineral Geochem* 54(1):329–356.
14. Riding R (2000) Microbial carbonates: The geological record of calcified bacterial–algal mats and biofilms. *Sedimentology* 47(s1):179–214.
15. Arp G, Reimer A, Reitner J (2001) Photosynthesis-induced biofilm calcification and calcium concentrations in Phanerozoic oceans. *Science* 292(5522):1701–1704.
16. Aloisi G (2008) The calcium carbonate saturation state in cyanobacterial mats throughout Earth's history. *Geochim Cosmochim Acta* 72(24):6037–6060.
17. Shiraishi F (2012) Chemical conditions favoring photosynthesis-induced $CaCO_3$ precipitation and implications for microbial carbonate formation in the ancient ocean. *Geochim Cosmochim Acta* 77:157–174.
18. Perry RS, Mcloughlin N, Lynne BY, Sephton MA (2007) Defining biominerals and organominerals: Direct and indirect indicators of life. *Sediment Geol* 201(1-2):157–179.
19. Dupraz C, et al. (2009) Processes of carbonate precipitation in modern microbial mats. *Earth Sci Rev* 96(3):141–162.
20. Werner U, et al. (2008) Microbial photosynthesis in coral reef sediments (Heron Reef, Australia). *Estuar Coast Shelf Sci* 76(4):876–888.
21. Schoon R, Bissett A, De Beer D (2010) Resilience of pore-water chemistry and calcification in photosynthetic zones of calcifying sediments. *Limnol Oceanogr* 55(1):377–385.
22. LaJeunesse TC (2001) Investigating the biodiversity, ecology, and phylogeny of endosymbiotic dinoflagellates in the genus *Symbiodinium* using the ITS region: In search of a 'species' level marker. *J Phycol* 37(5):866–880.
23. Pochon X, Montoya-Burgos JI, Stadelmann B, Pawlowski J (2006) Molecular phylogeny, evolutionary rates, and divergence timing of the symbiotic dinoflagellate genus *Symbiodinium*. *Mol Phylogenet Evol* 38(1):20–30.
24. Thornton DC, Fejes EM, DiMarco SF, Clancy KM (2007) Measurement of acid polysaccharides in marine and freshwater samples using alcian blue. *Limnol Oceanogr Methods* 5:73–87.
25. Ries JB, Stanley SM, Hardie LA (2006) Scleractinian corals produce calcite, and grow more slowly, in artificial Cretaceous seawater. *Geology* 34(7):525–528.
26. Sarmiento JL, Gruber N (2006) *Ocean Biogeochemical Dynamics* (Princeton Univ Press, Princeton, NJ).
27. Frommlet JC, Guimarães B, Sousa L, Serôdio J, Alves A (2015) *Neptunomonas phycophila* sp. nov. isolated from a culture of *Symbiodinium* sp., a dinoflagellate symbiont of the sea anemone *Aiptasia tagetes*. *Int J Syst Evol Microbiol* 65(Pt 3):915–919, 10.1099/ijs.0.000039.
28. Uhlinger DJ, White DC (1983) Relationship between physiological status and formation of extracellular polysaccharide glycocalyx in *Pseudomonas atlantica*. *Appl Environ Microbiol* 45(1):64–70.
29. Shiraishi F, Bissett A, De Beer D, Reimer A, Arp G (2008) Photosynthesis, respiration and exopolymer calcium-binding in biofilm calcification (Westerhöfer and Deinschwanger Creek, Germany). *Geomicrobiol J* 25:83–94.
30. Provasoli L, McLaughlin JJA, Droop MR (1957) The development of artificial media for marine algae. *Arch Mikrobiol* 25(4):392–428.
31. Blank RJ (1987) Cell architecture of the dinoflagellate *Symbiodinium* sp. inhabiting the Hawaiian stony coral *Montipora verrucosa*. *Mar Biol* 94(1):143–155.
32. Santos SR, Taylor DJ, Coffroth MA (2001) Genetic comparisons of freshly isolated versus cultured symbiotic dinoflagellates: Implications for extrapolating to the intact symbiosis. *J Phycol* 37(5):900–912.
33. Hoppenrath M, Murray SA, Chomérat N, Horiguchi T, eds (2014) *Marine Benthic Dinoflagellates - Unveiling their Worldwide Biodiversity* (Schweizerbart'sche Verlagsbuchhandlung, Stuttgart).
34. Jeong HJ, et al. (2014) Feeding by heterotrophic dinoflagellates and ciliates on the free-living dinoflagellate *Symbiodinium* sp. (Clade E). *J Eukaryot Microbiol* 61(1):27–41.
35. Friedmann EI (1982) Endolithic microorganisms in the antarctic cold desert. *Science* 215(4536):1045–1053.
36. Shashar N, Banaszak AT, Lesser MP, Amrami D (1997) Coral endolithic algae: Life in a protected environment. *Pac Sci* 51(2):167–173.
37. Taylor FJR, Pollingher U (1987) Ecology of dinoflagellates. *The Biology of Dinoflagellates*, ed Taylor FJR (Blackwell, Oxford, UK), pp 398–502.
38. Siano R, Montresor M, Probert I, Not F, de Vargas C (2010) *Pelagodinium* gen. nov. and *P. béii* comb. nov., a dinoflagellate symbiont of planktonic foraminifera. *Protist* 161(3):385–399.
39. Malcolm H, April H (2012) The magnesium inhibition and arrested phagosome hypotheses: New perspectives on the evolution and ecology of *Symbiodinium* symbioses. *Biol Rev Camb Philos Soc* 87(4):804–821.
40. Riding R, Liang L (2005) Geobiology of microbial carbonates: Metazoan and seawater saturation state influences on secular trends during the Phanerozoic. *Palaeogeogr Palaeocl* 219(1-2):101–115.
41. Guillard RRL (1975) Culture of phytoplankton for feeding marine invertebrates. *Culture of Marine Invertebrate Animals*, eds Smith WL, Chanley MH (Plenum, New York), pp 29–60.
42. Brading P, et al. (2011) Differential effects of ocean acidification on growth and photosynthesis among phylotypes of *Symbiodinium* (Dinophyceae). *Limnol Oceanogr* 56(3):927–938.
43. Gran G (1950) Determination of the equivalence point in potentiometric titrations. *Acta Chem Scand* 4:559–577.
44. Gran G (1952) Determination of the equivalence point in potentiometric titrations. part II. *Analyst (Lond)* 77:661–671.
45. Rounds SA (2009) Alkalinity calculator. Version 2.22. Perl Program. or.water.usgs.gov/alk/.
46. Zurel D, Shaham O, Brickner I, Benayahu Y (2008) DAPI-based vital staining reveals entry of heterologous zooxanthellae into primary polyps of a vertically-transmitting soft coral. *Symbiosis* 46(3):145–151.
47. Jain R, Raghukumar S, Tharanathan R, Bhosle NB (2005) Extracellular polysaccharide production by thraustochytrid protists. *Mar Biotechnol (NY)* 7(3):184–192.
48. Schreiber U, Schliwa U, Bilger W (1986) Continuous recording of photochemical and non-photochemical chlorophyll fluorescence quenching with a new type of modulation fluorometer. *Photosynth Res* 10(1-2):51–62.
49. Serôdio J (2004) Analysis of variable chlorophyll fluorescence in microphytobenthos assemblages: Implications of the use of depth-integrated measurements. *Aquat Microb Ecol* 36:137–152.
50. Weisburg WG, Barns SM, Pelletier DA, Lane DJ (1991) 16S ribosomal DNA amplification for phylogenetic study. *J Bacteriol* 173(2):697–703.